

Electron-Phonon Coupling in Wurtzite Semiconductors: Intervalley Scattering Selection Rules for Hexagonal GaN

K. M. Borysenko,^{1,*} M. El-Batanouny,² and E. Bellotti¹

¹*Department of Electrical and Computer Engineering,
Boston University, Boston, Massachusetts 02215*

²*Department of Physics, Boston University, Boston, Massachusetts 02215*

(Dated: September 14, 2021)

Selection rules are presented for electron-phonon scattering in GaN with the wurtzite crystal structure. The results are obtained for the interband scattering between the lowest conduction band (Γ -valley) and the second conduction band (U -valley). These selection rules are derived based on the original group-theoretical analysis of the crystal vibrations in GaN, which included detailed compatibility relations for all phonon modes.

PACS numbers: 71.38.-k, 63.20.kd, 03.65.Fd

I. INTRODUCTION

Gallium nitride (GaN) and other group III nitrides have been playing an increasingly important role in modern electronics, optoelectronics, and photonics since 1990's; they are successfully competing with more conventional semiconductors in various applications. The wide band gap of these materials provides numerous advantages for device design. In particular, it makes them suitable for operating at high operating temperatures and electric field strengths in high-power and microwave electronics. Furthermore, because of the wide range of band band gap tunability, GaN-based alloys are also desirable for use in optoelectronics from the infrared to the blue and ultraviolet spectral range. One of the key requirements for further successful applications of GaN and its alloys, is better understanding of their carrier transport properties. A stepping stone toward this goal is the development of a comprehensive theory that describes carrier-phonon interaction processes.

Recently, there have been several theoretical studies of the electron-phonon coupling in hexagonal GaN¹⁻³, where the strength of the charge carrier interaction with the crystal lattice was estimated in the framework of the rigid pseudion model. While the results of these studies for the carrier transport are in reasonable agreement with the available experimental data, a more comprehensive theoretical underpinning is still required. Presently, experimental results specific to the electron-phonon interaction processes in GaN are scarce and it is crucial to have an independent and reliable way of validating new theoretical predictions.

Group theory provides a unique approach to establish this theoretical basis since it allows drawing important and far-reaching conclusions on the characteristics of the electron-phonon interaction

processes based solely on very general symmetry properties of the participating electron states and phonon modes. Particularly, it allows one to establish which carrier-phonon scattering scenarios are permitted or prohibited by symmetry.

In this work, we use the group-theoretical approach in order to obtain detailed selection rules for the electron-phonon scattering in the wurtzite GaN, in the same spirit as it has been done for other materials, such as diamond⁴ and, more relevantly, III-V semiconductors with the cubic zincblends crystal structure⁵. It is noteworthy that certain selection rules for GaN are already available in the literature; however these works focus on optical transitions and Raman effect⁶⁻⁹. In this work, on the other hand, we derive the selection rules specifically for the electron scattering between the two lowest conduction bands of GaN, which is a key to a better understanding of the charge carrier transport in this semiconductor. We consider the wurtzite GaN, a predominant crystal structure.

In order to obtain the selection rules for phonon-mediated electron transitions, one has to (i) derive compatibility relations for all irreducible representations (irreps) that describe the symmetry of each phonon mode, for all high-symmetry points and lines in the (BZ); (ii) establish which irreps describe the symmetry of the electron states before and after scattering; (iii) based on the results of the first two steps, apply a well-known relation from the group theory (see Eq. (5)) in order to find which scattering scenarios are allowed. Additionally, when one considers the electrons in a certain valley of a conduction or valence band, the compatibility relations for irreps that characterize the electron states in the vicinity of the corresponding extremum point are also necessary for a full picture. We describe these three stages and the key results in the following sections.

II. THE SYMMETRY OF ELECTRON STATES AND COMPATIBILITY RELATIONS FOR PHONON MODES

Crystal symmetry determines the classification of both electron states and phonon modes^{20,21}. The general symmetry properties of the wurtzite crystal structure have been studied since as early as 1950's²²; it has been found that it consists of two interpenetrating close-packed lattices separated by $u = 3/8c$ along the z -direction, where c is the lattice constant perpendicular to the xy -plane. This crystal structure is described by the space group $\mathbb{G} = C_{6v}^4$, which is a non-symmorphic group with 12 coset representatives with respect to the translation group \mathbb{T} ; half of these twelve elements are symmorphic ($\{E|0\}, 2\{C_3|0\}, 3\{\sigma_d^{(i)}|0\}$) and the other half ($\{C_2|\tau\}, 2\{C_6|\tau\}, 3\{\sigma_v^{(i)}|\tau\}$) include an improper translation $\tau = (c/2)\hat{z}$. Fig. 1(a) shows the projection of the wurtzite crystal lattice onto the xy -plane, with all its symmetry elements.

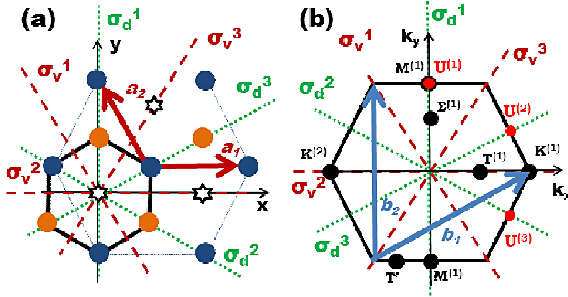


FIG. 1: (Color online) (a) The projection of the wurtzite lattice on xy -plane. \mathbf{a}_1 and \mathbf{a}_2 are two independent translation vectors on xy -plane. The solid (black) line shows the borders of the symmetrized (Wigner-Seitz) unit cell. The locations of all symmetry elements on the plane are also shown: six-fold (screw) axes are marked by six-point stars; glide planes are shown as dashed (red) lines; three regular reflection planes are marked by dotted (green) lines. (b) The Brillouin zone (BZ) of the wurtzite crystal. Two reciprocal lattice vectors in $k_x k_y$ -plane (\mathbf{b}_1 and \mathbf{b}_2) are shown as blue arrows. All major points of high symmetry on this plane are marked by black dots. The projections of the three non-equivalent vectors of the star of $\mathbf{q} = U$ are also shown as smaller (red) dots. Superscripts indicate different vectors in the same star (e.g., the point K , whose star has two vectors, $K^{(1)}$ and $K^{(2)}$).

A simplification of the analysis is achieved in the case of the wurtzite structure if we select the origin of coordinates on xy -plane, at the point where it is crossed by the six-fold rotational axis C_6 (as it is pictured on Fig. 1(a)) rather than at an atomic

site²³. The lattice basis vectors are given by

$$\begin{cases} \mathbf{a}_1 = a \hat{\mathbf{x}}, \\ \mathbf{a}_2 = \frac{a}{2} (-\hat{\mathbf{x}} + \sqrt{3} \hat{\mathbf{y}}), \\ \mathbf{a}_3 = c \hat{\mathbf{z}} \end{cases} \quad (1)$$

The atomic basis coordinates (in terms of \mathbf{a}_1 - \mathbf{a}_3) are

$$\begin{aligned} \boldsymbol{\rho}_1^{\text{Ga}} &= \left(\frac{1}{3}, \frac{2}{3}, 0\right), & \boldsymbol{\rho}_2^{\text{Ga}} &= \left(\frac{2}{3}, \frac{1}{3}, \frac{1}{2}\right) \\ \boldsymbol{\rho}_1^{\text{N}} &= \left(\frac{1}{3}, \frac{2}{3}, u\right), & \boldsymbol{\rho}_2^{\text{N}} &= \left(\frac{2}{3}, \frac{1}{3}, \frac{1}{2} + u\right) \end{aligned}$$

where $u = 3/8c$. Fig. 1(b) shows the reciprocal space with the Brillouin zone (BZ) that corresponds to this choice of coordinates. The reciprocal basis vectors are

$$\begin{cases} \mathbf{b}_1 = \frac{2\pi}{a} \left(\hat{\mathbf{x}} + \frac{1}{\sqrt{3}} \hat{\mathbf{y}}\right); \\ \mathbf{b}_2 = \frac{4\pi}{\sqrt{3}a} \hat{\mathbf{y}}; \\ \mathbf{b}_3 = \frac{2\pi}{c} \hat{\mathbf{z}}. \end{cases} \quad (2)$$

The M - and K -point wavevectors are

$$\mathbf{k}_M = \frac{2\pi}{\sqrt{3}a} \hat{\mathbf{y}}; \quad \mathbf{k}_K = \frac{4\pi}{3a} \hat{\mathbf{x}}.$$

Before we proceed with the discussion of our findings, it is important to mention the issue of inconsistent notations that appear in the literature for wurtzite type crystals, as well as in the published character tables for space groups^{16-20,22}. This problem has been discussed before^{14,24} and the authors of the Ref. 14 have done a thorough comparison of the various existing notations. For the sake of consistency, we will use the tables of characters from the Ref. 16 throughout this work. The reader interested in the symmetry properties of the wurtzite crystal structure should be aware of the discrepancies in the nomenclature of irreps used by different authors, in order to avoid the confusion. One important case in point is the group of the wave vector $\mathbf{q}_\Gamma = (0,0,0)$ isomorphic to the point group C_{6v} , which has six irreps Γ_i ($i = 1, \dots, 6$). Comparison of the character tables¹⁴ shows that one of the irreps pertinent to our analysis, namely Γ_4 , is labelled as Γ_3 in a number of recent works^{9,13}. At the same time, molecular spectroscopy notations (See, for example tables in Ref. 20) remain popular in the literature^{25,28-30}; in this alternative convention, Γ_4 is commonly labelled as B_1 . Aside from the identity representation Γ_1 , the one-dimensional irrep relevant for the hexagonal GaN is the one with characters (-1) for each non-symmorphic operation (i.e., $\{C_2|\tau\}, 2\{C_6|\tau\}, 3\{\sigma_v^{(i)}|\tau\}$). Lastly, we emphasize

that the difference between the character tables of Γ_3 and Γ_4 is that the characters of the glide planes $\sigma_v^{(i)}$ and the regular planes $\sigma_d^{(i)}$ exchange signs.

The s-like²⁶ lowest and the second lowest conduction bands (CB1 and CB2, respectively) are non-degenerate throughout the entire BZ²⁷. They have been identified in an early study of the electronic structure of GaN¹⁰ as belonging to the irreps Γ_1 (CB1) and Γ_4 (CB2). More recent theoretical^{9,14,26} and experimental¹¹⁻¹³ studies confirm these results. The electronic state at the minimum of the U -valley has a symmetry U_2 , compatible with Γ_4 ^{10,11}. The compatibility relations for the electron states near the bottoms of the two conduction bands are shown on Fig. 2.

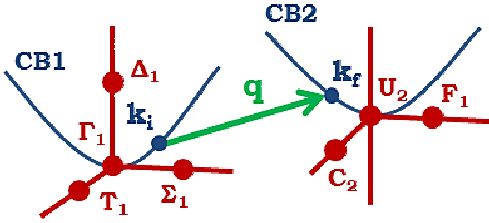


FIG. 2: (Color online) Compatibility relations for the electron states in two lowest conduction bands (CB1 and CB2). The green arrow signifies an arbitrary electron scattering that involves a phonon with a wave vector $\mathbf{q} = \mathbf{k}_f - \mathbf{k}_i$.

Having established the symmetry of the relevant electron states in hexagonal GaN, it is now necessary to comprehensively describe the symmetry of atomic thermal vibrations in wurtzite. This implies deriving compatibility relations between all points of high symmetry in the BZ. Generally, these relations allow for several equally valid solutions. For example, as $\mathbf{q}_\Sigma \rightarrow \mathbf{q}_M$, the compatibility relations are

$$\Sigma_1 \rightarrow M_1, M_4; \Sigma_2 \rightarrow M_2, M_3.$$

Therefore, if a certain phonon branch's symmetry is described by Σ_1 along the Σ -direction, one has to still establish which of the two compatible irreps describes that branch at the M -point. To eliminate such ambiguity, we have obtained symmetry-adapted vectors for atomic displacements in the wurtzite crystal at the Γ -point (The procedure for obtaining these vectors, based on symmetry projection operators, is described in detail in Chapter 6 of Ref. 21). The phonon polarization vectors at a given \mathbf{q} -point of the BZ can be readily obtained by constructing normalized linear combinations of the symmetry-adapted vectors. The resulting vectors for the Γ -point can be found in Appendix A.

Three acoustic phonon modes are easily identified among the obtained vectors as:

$$\begin{cases} |\Gamma^{(ac)}, x\rangle = |5, 1\rangle, \\ |\Gamma^{(ac)}, y\rangle = |5, 3\rangle, \\ |\Gamma^{(ac)}, z\rangle = |1, 1\rangle, \end{cases} \quad (3)$$

(See Eqs. (A1a)-(A3d)), in agreement with Ref. 15 which assigns $\Gamma_1 \oplus \Gamma_5$ to three acoustic phonon modes at the point Γ . The remaining vectors in Eqs. (A1a)-(A4d) also agree with atomic displacement patterns for optical modes published earlier²⁵. By applying this procedure to all pertinent points of high symmetry we generate all polarization vectors, as well as compatible irrep frequencies a_i . The following relations show how the reducible representation D that describes *all* atomic displacements in the wurtzite crystal, splits into compatible irreps in all major points of high symmetry on the $k_x k_y$ -plane in the BZ:

$$D^\Gamma = 2\Gamma_1 \oplus 2\Gamma_4 \oplus 2\Gamma_5 \oplus 2\Gamma_6, \quad (4a)$$

$$D^T = 6T_1 \oplus 6T_2, \quad (4b)$$

$$D^K = 2K_1 \oplus 2K_2 \oplus 4K_3, \quad (4c)$$

$$D^\Sigma = 8\Sigma_1 \oplus 4\Sigma_2, \quad (4d)$$

$$D^M = 4M_1 \oplus 2M_2 \oplus 2M_3 \oplus 4M_4, \quad (4e)$$

$$D^{T'} = 6T'_1 \oplus 6T'_2. \quad (4f)$$

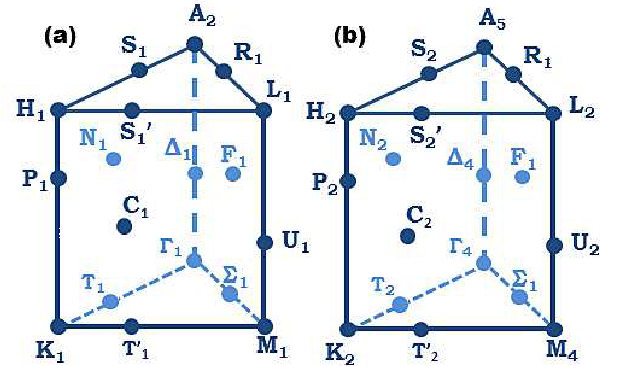


FIG. 3: Compatibility relations for the phonon modes Γ_1 (a) and Γ_4 (b) in the irreducible wedge of the BZ. All irrep labels correspond to the convention used in the character tables in Ref. 16. An arbitrary point in the bulk of the irreducible wedge Θ'_1 , is not shown as it does not have any symmetry operations associated with it and is irrelevant to the selection rules discussed in this work.

Since no group of a wave vector in the BZ of the wurtzite crystal contains operations that affect z -component of \mathbf{q} ,²² the phonon modes with the same (q_x, q_y) have the same symmetry-adapted

vectors associated with them. In other words, polarization vectors $\mathbf{e}_\mu(\mathbf{q})$ that determine atomic displacements for each mode $\mu = 1, \dots, 12$, are independent of q_z . The summary of the obtained compatibility relations is presented on Figs. (3-5). To the best of our knowledge, the only work that has previously shown detailed compatibility relations was Ref. 15, which studied the phonon spectrum of CdS with the wurtzite crystal structure. These results should be completely applicable to any crystal with the wurtzite structure. However, a careful analysis reveals several inconsistencies in the compatibility relations of Ref. 15. Particularly, they do not agree with the results of Eqs. (4a-4f). The recalculated compatibility relations shown on Figs. (3-5) resolve this issue.

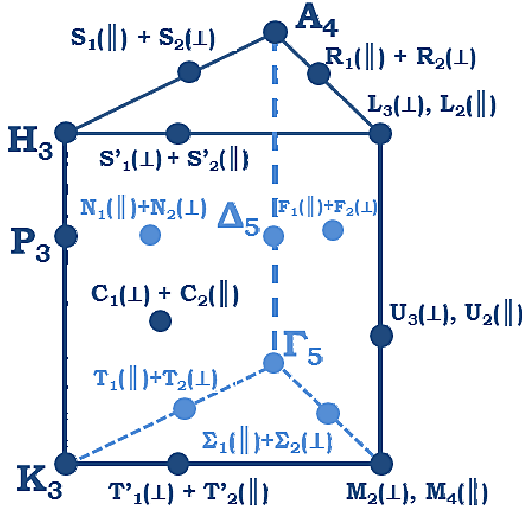


FIG. 4: Compatibility relations for the phonon mode Γ_5 in the irreducible wedge of the BZ. A symbol \parallel (\perp) next to the name of an irrep signifies that the latter describes a mode at a given point \mathbf{q} , with the polarization vector parallel (perpendicular) to the reflection plane in which the vector \mathbf{q} lies. Symbols with a larger font (e.g., Δ_5) mark the points inside the BZ where two phonon modes are allowed to be degenerate by symmetry and thus, are described by two-dimensional irreps. Note that the plus sign is used whenever a certain point is adjacent to one where two modes are degenerate by symmetry; therefore, it emphasizes that the degeneracy is lifted due to a reduced symmetry.

III. SELECTION RULES

A selection rule in the case of electron-phonon interaction provides an answer to a question whether the Kronecker product of three irreps $\left([D_\gamma^{\mathbf{k}_f}]^* \otimes D_\beta^{\mathbf{q}} \otimes D_\alpha^{\mathbf{k}_i}\right)$ contains the identity repre-

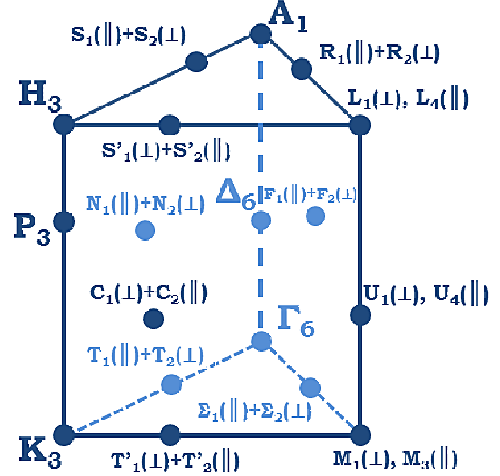


FIG. 5: Compatibility relations for the phonon mode Γ_6 in the irreducible wedge of the BZ. See also the caption to Fig. 4.

sentation, where $D_\alpha^{\mathbf{k}_i}$, $D_\gamma^{\mathbf{k}_f}$, and $D_\beta^{\mathbf{q}}$ are the representations of, respectively, the group of the wave vector of the electron $G^{\mathbf{k}_i}$ (initial state, i.e., before scattering), $G^{\mathbf{k}_f}$ (final state), and the phonon $G^{\mathbf{q}}$ involved in scattering ($\mathbf{q} = \mathbf{k}_f - \mathbf{k}_i$, by momentum conservation). If the answer is positive, then such scattering process is allowed by symmetry. Formally, one has to find the frequency of the identity representation for each combination of three irreps $D_\alpha^{\mathbf{k}_i}$, $D_\gamma^{\mathbf{k}_f}$, and $D_\beta^{\mathbf{q}}$, according to the well-known relation^{20,21}

$$a_1 = \frac{1}{h} \sum_{g \in (G^{\mathbf{k}_f} \cap G^{\mathbf{q}} \cap G^{\mathbf{k}_i})} [\chi_\gamma^{\mathbf{k}_f}(g)]^* \chi_\beta^{\mathbf{q}}(g) \chi_\alpha^{\mathbf{k}_i}(g), \quad (5)$$

where h is the number of elements in the group $(G^{\mathbf{k}_f} \cap G^{\mathbf{q}} \cap G^{\mathbf{k}_i})$, and $\chi_\alpha^{\mathbf{k}} = \text{Tr} [D_\alpha^{\mathbf{k}}]$ is the character of the α th irrep of the wave group of \mathbf{k} , $D_\alpha^{\mathbf{k}}$. If $a_1 = 0$ for chosen $D_\alpha^{\mathbf{k}_i}$, $D_\gamma^{\mathbf{k}_f}$, and $D_\beta^{\mathbf{q}}$, then such scattering scenario is prohibited by symmetry.

A summary of all non-trivial selection rules for the interband scattering (CB1-CB2) between Γ - and U -valleys in hexagonal GaN is presented in Table I. Three sections of the table show scattering scenarios for three high-symmetry points/directions in Γ -valley of CB1: Γ , Σ , and T . Each row in a table represents a specific scattering process, when the initial and final electron states are defined. Note that the selection rules for the initial electron state with the wave vector $\mathbf{k} = (k_x, k_y, k_z)$ are exactly the same as for the case when this vector is projected on xy -plane: $\mathbf{k}' = (k_x, k_y, 0)$. So for example, electron scattering from a Δ -point follows the same rules as scattering

from $\mathbf{k} = \Gamma$. Ultimately, this is due to the property mentioned earlier, that all symmetry operations of the wurtzite type crystal leave z -component of the wave vector unchanged.

Finally, one can think of more scattering scenarios between Γ - and U -valleys than what is presented in the Table I, due to all possible combinations of vectors in the stars of \mathbf{q} and \mathbf{k}_f (we can assume that \mathbf{k}_i is fixed). However, analysis reveals that many of these combinations correspond to the same (lowest symmetry) case when the intersection of the groups ($G^{\mathbf{k}_f} \cap G^{\mathbf{q}} \cap G^{\mathbf{k}_i}$) contains only one element, $\{E|0\}$ and thus, according to Eq. (5) all phonon modes in wurtzite GaN can participate in such scattering process. All these cases are excluded from the Table I as trivial, with the exception of the last row of the case (II). The latter illustrates the situation when three groups of the wave vectors $G^{\mathbf{k}_f}$, $G^{\mathbf{q}}$, and $G^{\mathbf{k}_i}$, while generally possessing certain symmetries individually ($\{\sigma_d^1|0\} \in G^{\mathbf{k}_i}$, $\{\sigma_v^2|\tau\} \in G^{\mathbf{k}_f}$, $\{\sigma_v^3|\tau\} \in G^{\mathbf{q}}$), have no common symmetry operations except the identity $\{E|0\}$.

IV. CONCLUSIONS

In this work, we have derived the selection rules for electron scattering between the two conduction bands in the wurtzite GaN. This analysis is based on the detailed compatibility relations for all phonon modes, which revealed some inconsistencies in the earlier work¹⁵. Due to a relatively low symmetry of the wurtzite crystal structure, a majority of the phonon modes are allowed to participate in the electron scattering between the valleys at $\mathbf{q} = \Gamma$ (CB1) and $\mathbf{q} = U$ (CB2), with the exception of the z -polarized Γ_1 -modes (both acoustic and optical), which have shown a number of restrictions along high-symmetry directions of the BZ. Parallel-vs-perpendicular nature of the modes (i.e. whether a given polarization vector is parallel or perpendicular to a reflection plane that contains the vector \mathbf{q}) also imposes certain restrictions in case of the phonons described by the irreps Γ_5 and Γ_6 . These results provide a reliable sanity check for future theoretical studies that involve electron-phonon coupling in hexagonal GaN, as they are expected to dictate the overall behavior of the corresponding matrix elements.

V. ACKNOWLEDGMENT

KMB and EB gratefully acknowledge financial support from the U. S. Army Research Laboratory through the Collaborative Research Alliance

TABLE I: A summary of the selection rules for the case when the electron is being scattered by a phonon from the Γ -valley in CB1, to the U -valley in CB2. Three specific points in CB1 are considered: (I) Γ -point (or a Δ -point); (II) Σ -point (or an F -point) ; (III) T -point (or an N -point). The subscripts identify the irreps that describe the symmetry of the electron states and the phonon mode involved in the scattering process. The superscript (e.g., in $U_2^{(3)}$) specifies which vector in the star $S_{\mathbf{q}}$ is being considered (See Fig. 1(b)). The notation $\{U_2\}$ is used for the minimum of the U -valley together with its neighborhood. The first column shows the irrep that describes the final electron state. The second column shows which phonon irrep $D_{\beta}^{\mathbf{q}}$ (with $\mathbf{q} = \mathbf{k}_f - \mathbf{k}_i$) is allowed by selection rules for the specified initial and final electron states. The last column shows which phonon modes of wurtzite GaN are compatible with a given $D_{\beta}^{\mathbf{q}}$. Since only one final state ($U_2^{(1)}$ (or $C_2^{(1)}$, which leads to the same selection rules)) is considered in case (III), the first column in this section is left empty.

(I)		$D_{\alpha}^{\mathbf{k}_i} = \Gamma_1$	$\xrightarrow{D_{\beta}^{\mathbf{q}}}$	$D_{\gamma}^{\mathbf{k}_f} = \{U_2\}$
$D_{\gamma}^{\mathbf{k}_f}$	$D_{\beta}^{\mathbf{q}}$	Allowed modes		
U_2	U_2	$ 4, \{1, 2\}\rangle, 5, \{3, 4\}\rangle$		
F_1	F_1	$ 1, \{1, 2\}\rangle, 4, \{1, 2\}\rangle, 5, \{3, 4\}\rangle, 6, \{3, 4\}\rangle$		
C_2	C_2	$ 4, \{1, 2\}\rangle, 5, \{3, 4\}\rangle, 6, \{1, 2\}\rangle$		
(II)		$D_{\alpha}^{\mathbf{k}_i} = \Sigma_1^{(1)}$	$\xrightarrow{D_{\beta}^{\mathbf{q}}}$	$D_{\gamma}^{\mathbf{k}_f} = \{U_2^{(1)}\}$
$D_{\gamma}^{\mathbf{k}_f}$	$D_{\beta}^{\mathbf{q}}$	Allowed modes		
U_2	F_1	$ 1, \{1, 2\}\rangle, 4, \{1, 2\}\rangle, 5, \{3, 4\}\rangle, 6, \{3, 4\}\rangle$		
F_1	F_1	$ 1, \{1, 2\}\rangle, 4, \{1, 2\}\rangle, 5, \{3, 4\}\rangle, 6, \{3, 4\}\rangle$		
C_2	$N_{1,2}$	All modes are allowed		
(III)		$D_{\alpha}^{\mathbf{k}_i} = T_1^{(1)}$	$\xrightarrow{D_{\beta}^{\mathbf{q}}}$	$D_{\gamma}^{\mathbf{k}_f} = U_2^{(1)}(C_2^{(1)})$
$D_{\gamma}^{\mathbf{k}_f}$	$D_{\beta}^{\mathbf{q}}$	Allowed modes		
	C_2	$ 4, \{1, 2\}\rangle, 5, \{3, 4\}\rangle, 6, \{1, 2\}\rangle$		
	$P_{2,3}$	$ 4, \{1, 2\}\rangle, 5, \{1, \dots, 4\}\rangle, 6, \{1, \dots, 4\}\rangle$		

(CRA) for MultiScale multidisciplinary Modeling of Electronic materials (MSME).

Appendix A: Polarization vectors of the phonon modes in the wurtzite crystal

The following is a list of the twelve phonon polarization vectors at the point Γ , divided among

four different irreps (See Eq. (4a)):

$$2\Gamma_1 : \\ |1, 1\rangle = \frac{1}{2} \{\hat{z}, \hat{z}, \hat{z}, \hat{z}\}, \quad (\text{A1a})$$

$$|1, 2\rangle = \frac{1}{2} \{\hat{z}, \hat{z}, -\hat{z}, -\hat{z}\}, \quad (\text{A1b})$$

$$2\Gamma_4 : \\ |4, 1\rangle = \frac{1}{2} \{-\hat{z}, \hat{z}, -\hat{z}, \hat{z}\}, \quad (\text{A2a})$$

$$|4, 2\rangle = \frac{1}{2} \{-\hat{z}, \hat{z}, \hat{z}, -\hat{z}\}, \quad (\text{A2b})$$

$$2\Gamma_5 : \\ |5, 1\rangle = \frac{1}{2} \{\hat{x}, \hat{x}, \hat{x}, \hat{x}\}, \quad (\text{A3a})$$

$$|5, 2\rangle = \frac{1}{2} \{\hat{x}, \hat{x}, -\hat{x}, -\hat{x}\}, \quad (\text{A3b})$$

$$|5, 3\rangle = \frac{1}{2} \{\hat{y}, \hat{y}, \hat{y}, \hat{y}\}, \quad (\text{A3c})$$

$$|5, 4\rangle = \frac{1}{2} \{\hat{y}, \hat{y}, -\hat{y}, -\hat{y}\}, \quad (\text{A3d})$$

$$2\Gamma_6 : \\ |6, 1\rangle = \frac{1}{2} \{-\hat{x}, \hat{x}, -\hat{x}, \hat{x}\}, \quad (\text{A4a})$$

$$|6, 2\rangle = \frac{1}{2} \{-\hat{x}, \hat{x}, \hat{x}, -\hat{x}\}, \quad (\text{A4b})$$

$$|6, 3\rangle = \frac{1}{2} \{-\hat{y}, \hat{y}, -\hat{y}, \hat{y}\}, \quad (\text{A4c})$$

$$|6, 4\rangle = \frac{1}{2} \{-\hat{y}, \hat{y}, \hat{y}, -\hat{y}\}. \quad (\text{A4d})$$

These vectors are 12-dimensional (four atoms in the wurtzite unit cell, times three Cartesian coordinates). We, however, use a more compact, four-component notation, where the displacement of each of four atoms of the basis is described by an appropriate unit vector. So for instance, an atomic displacement along x-direction is described by the vector $\hat{x} = (1, 0, 0)$. These twelve vectors represent all possible atomic displacement patterns in the wurtzite crystal. They form a basis that spans the corresponding Hilbert space, so that any phonon

mode at a point $\mathbf{q} \neq \Gamma$ of the BZ can also be represented in terms of these vectors. In other words, Eqs. (A1a-A4d) define basis functions for *all* compatible irreps at different points in the BZ of the wurtzite crystal. Table II shows a list of all compatible irreps (See Figs. (3-5)) for high-symmetry \mathbf{q} -points in $q_x q_y$ -plane, with corresponding polarization vectors. This table, together with the vectors (A1a-A4d) and the frequencies of irreps at different points of the BZ (See Eqs. (4a-4f)), provides

TABLE II: A list of high-symmetry points on $q_x q_y$ -plane of the BZ of wurtzite (first column), with associated irreps (second column; see also Figs. (3-5)), and corresponding polarization vectors (third column). The superscripts in the names of the high-symmetry points indicate the choice of the vector in the star (See Fig. 1). If several eigenvectors $|\alpha, i\rangle, \dots, |\alpha, j\rangle$ of an irrep Γ_α serve as basis functions for an irrep specified in the second column, their full list is shown in curly braces: $|\alpha, \{i, \dots, j\}\rangle$.

$\Sigma^{(1)}$	Σ_1	$ 1, \{1, 2\}\rangle, 4, \{1, 2\}\rangle, 5, \{3, 4\}\rangle, 6, \{3, 4\}\rangle$
	Σ_2	$ 5, \{1, 2\}\rangle, 6, \{1, 2\}\rangle$
$M^{(1)}$	M_1	$ 1, \{1, 2\}\rangle, 6, \{3, 4\}\rangle$
	M_2	$ 5, \{1, 2\}\rangle$
	M_3	$ 6, \{1, 2\}\rangle$
	M_4	$ 4, \{1, 2\}\rangle, 5, \{3, 4\}\rangle$
$T^{(1)}$	T_1	$ 1, \{1, 2\}\rangle, 5, \{1, 2\}\rangle, 6, \{3, 4\}\rangle$
	T_2	$ 4, \{1, 2\}\rangle, 5, \{3, 4\}\rangle, 6, \{1, 2\}\rangle$
$K^{(1)}$	K_1	$ 1, \{1, 2\}\rangle$
	K_2	$ 4, \{1, 2\}\rangle$
	K_3	$ 5, \{1, \dots, 4\}\rangle, 6, \{1, \dots, 4\}\rangle$

a comprehensive picture of the symmetry of thermal atomic vibrations in the wurtzite GaN. Note that it is sufficient to consider only points in $q_x q_y$ -plane, since all modes on the same phonon branch and with the same (q_x, q_y) are characterized by the same polarization vectors (See the brief discussion at the end of Section II, in regards to Ref. 22).

* Email: kboryse@ncsu.edu

¹ S. Yamakawa, R. Akis, N. Faralli, M. Saraniti, S. M. Goodnick, J. Phys.: Condens. Matter **21** 174206 (2009).

² F. Bertazzi, M. Moresco, and E. Bellotti, J. Appl. Phys. **106**, 063718 (2009).

³ Michele Moresco, Francesco Bertazzi, and Enrico

Bellotti J. Appl. Phys. **106**, 063719 (2009).

⁴ J. L. Birman, Phys. Rev. **127**, 4, 1093-1106 (1962).

⁵ J. L. Birman, M. Lax, R. Loudon, Phys. Rev. **145**, 2, 620622 (1966).

⁶ J. L. Birman, Phys. Rev. **114**, 6, 1490-1492 (1959).

⁷ H. W. Streitwolf, Phys. Stat. Sol. **33**, 1, 225-233 (1969).

- ⁸ P. Tronc, Yu. E. Kitaev, G. Wang, M.F. Limonov, G. Neu, *Physica B*, **302303**, 291298 (2001).
- ⁹ Yu. E. Kitaev and P. Tronc, *Phys. Rev. B* **64**, 3, 205312-205323 (2001).
- ¹⁰ S. Bloom, G. Harbeke, E. Meier, I. B. Ortenburger, *Phys. Stat. Sol. (b)* **66**, 1, 161-168 (1974).
- ¹¹ W. R. L. Lambrecht, B. Segall, J. Rife, W. R. Hunter, and D. K. Wickenden, *Phys. Rev. B* **51**, 13516-13532 (1995).
- ¹² E. G. Brazel, M. A. Chin, V. Narayanamurti, D. Kapolnek, E. J. Tarsa, and S. P. DenBaars, *Appl. Phys. Lett.* **70**, 330 (1997).
- ¹³ N. Nepal, K. B. Nam, J. Li, M. L. Nakarmi, J. Y. Lin, and H. X. Jiang, *Appl. Phys. Lett.* **88**, 261919 (2006).
- ¹⁴ A. Marnetto, M. Penna, and M. Goano, *J. Appl. Phys.* **108**, 033701 (2010).
- ¹⁵ M. A. Nusimovici and J. L. Birman, *Phys. Rev.* **156**, 3, 925-938 (1967).
- ¹⁶ *The Irreducible representations of space groups*, Edited by J. Zak, W. A. Benjamin, Inc., New York (1969).
- ¹⁷ J. C. Slater, *Symmetry and Energy Bands in Crystals*, Dover (1973).
- ¹⁸ A. P. Cracknell, B. L. Davies, S. C. Miller, and W. F. Love, *Kronecker Product Tables*, Plenum, New York, (1979).
- ¹⁹ *Light Scattering in Solids II, Basic Concepts and Instrumentation*, Edited by M. Cardona and G. Güntherodt, Topics in Applied Physics, Volume 50 (1982).
- ²⁰ M. Tinkham, *Group Theory and Quantum Mechanics*, Dover Publications (2003).
- ²¹ M. El-Batanouny, F. Wooten, *Symmetry and Condensed Matter Physics: A Computational Approach*, Cambridge University Press (2008).
- ²² E.I. Rashba, *Sov. Phys. Solid. State*, **1**, 368-380 (1959).
- ²³ R. C. Casella, *Phys. Rev.* **114**, 6, 1514-1518 (1959).
- ²⁴ L. Patrick, D. R. Hamilton, and W. J. Choyke, *Phys. Rev.* **143**, 2, 526-536 (1966).
- ²⁵ I. Gorczyca, N. E. Christensen, E. L. Peltzer y Blanca, and C. O. Rodriguez, *Phys. Rev. B* **51**, 11936-11939 (1995).
- ²⁶ M. Suzuki, T. Uenoyama, A. Yanase, *Phys. Rev. B* **52**, 8132-8139 (1995).
- ²⁷ Their degeneracy on the surface of the BZ that contains the triangle $A - H - L$ can be explained by symmetry with respect to time reversal, in full analogy with what is observed in the phonon spectrum of the wurtzite crystal²⁴
- ²⁸ J. Zi, X. Wan, G. Wei, K. Zhang and X. Xie, *J. Phys.: Condens. Matter* **8**, 6323-6328 (1996).
- ²⁹ H. Siegle, G. Kaczmarczyk, L. Filippidis, A. P. Litvinchuk, A. Hoffmann, and C. Thomsen, *Phys. Rev. B* **55**, 7000-7004 (1997).
- ³⁰ K. Karch, J.-M. Wagner, and F. Bechstedt, *Phys. Rev. B* **57**, 12, 7043-7049 (1998).
- ³¹ C. Bungaro, K. Rapcewicz, and J. Bernholc, *Phys. Rev. B* **61**, 10, 6720-6725 (2000).